Id proteins promote a cancer stem cell phenotype in triple negative breast cancer via Robo1-dependent c-Myc activation

Wee S. Teo[1,2], Holly Holliday[1,2*], Nitheesh Karthikeyan[3*], Aurélie S. Cazet[1,2], Daniel L. Roden[1,2], Kate Harvey[1], Christina Valbirk Konrad[1], Reshma Murali[3], Binitha Anu Varghese[3], Archana P. T.[3,4], Chia-Ling Chan[1,2], Andrea McFarland[1], Simon Junankar[1,2], Sunny Ye[1], Jessica Yang[1], Iva Nikolic[1,2], Jaynish S. Shah[5], Laura A. Baker[1,2], Ewan K.A. Millar[1,6,7,8], Mathew J. Naylor[1,2,10], Christopher J. Ormandy[1,2], Sunil R. Lakhani[11], Warren Kaplan[1,12], Albert S. Mellick[13,14], Sandra A. O'Toole[1,9], Radhika Nair[1,2,3$], Alexander Swarbrick[1,2$].

Affiliations

[1]Garvan Institute of Medical Research, Darlinghurst, New South Wales, 2010, Australia
[2]St Vincent's Clinical School, Faculty of Medicine, UNSW Sydney, New South Wales, 2010, Australia
[3] Cancer Research Program, Rajiv Gandhi Centre for Biotechnology, Kerala, 695014, India
[4]Manipal Academy of Higher Education, Manipal, Karnataka, 576104, India
[5]Centenary Institute, The University of Sydney, New South Wales, 2050, Australia
[6] Department of Anatomical Pathology, NSW Health Pathology, St George Hospital, Kogarah NSW 2217 Australia
[7] School of Medical Sciences, UNSW Sydney, Kensington NSW 2033, Australia.
[8] School of Medicine, Western Sydney University, Locked Bag 1797, Penrith, NSW 2751, Australia
[9]Department of Tissue Pathology and Diagnostic Oncology, Royal Prince Alfred Hospital, Camperdown
[10]Discipline of Physiology & Bosch Institute, School of Medical Sciences, University of Sydney, NSW 2006
[11]The University of Queensland, UQ Centre for Clinical Research, School of Medicine and Pathology Queensland, The Royal Brisbane & Women's Hospital, Herston, Brisbane, Queensland 4029, Australia
[12]Peter Wills Bioinformatics Centre, Garvan Institute of Medical Research, Darlinghurst, NSW 2010, Australia
[13]UNSW Medicine, University of NSW, 18 High St, Kensington NSW 2052, Australia.
[14]Ingham Institute for Applied Medical Research, 1 Campbell Street, Liverpool, NSW 2170, Australia.

***** These authors contributed equally

$ Co-corresponding authors

$ Dr Radhika Nair
Present address
Rajiv Gandhi Centre for Biotechnology
Kerala, India
radhikanair@rgcb.res.in
Phone: +91-471-2781251

Fax: +91-471-2346333

$ A/Prof Alexander Swarbrick
Cancer Research Division, Garvan Institute of Medical Research
370 Victoria St, Darlinghurst, NSW, 2010
Australia
a.swarbrick@garvan.org.au
Phone: +61-2-9355-5780
Fax**:** +61-2-355-5869

Running title: Id-Robo1 axis controls CSC phenotypes in TNBC

Abstract

Breast cancers display phenotypic and functional heterogeneity. Several lines of evidence support the existence of cancer stem cells (CSCs) in certain breast cancers, a minor population of cells capable of tumor initiation and metastatic dissemination. Identifying factors that regulate the CSC phenotype is therefore important for developing strategies to treat metastatic disease. The Inhibitor of Differentiation Protein 1 (Id1) and its closely related family member Inhibitor of Differentiation 3 (Id3) are expressed by a diversity of stem and progenitor cells and are required for metastatic dissemination in experimental models of breast cancer. Here, we show that ID1 is expressed in rare neoplastic cells within ER-negative breast cancers and enriched in brain metastases compared to patient matched primary tissues. To address the function of Id1 expressing cells within tumors, we developed two independent murine models of Triple Negative Breast Cancer (TNBC) in which a genetic reporter permitted the prospective isolation of $Id1^+$ cells. $Id1^+$ cells are enriched for self-renewal in tumorsphere assays *in vitro* and for tumor initiation *in vivo*. Conversely, depletion of Id1 and Id3 in the 4T1 murine model of TNBC demonstrates that Id1/3 are required for cell proliferation and self-renewal *in vitro*, as well as primary tumor growth and metastatic colonization of the lung *in vivo*. We defined a novel mechanism of Id protein function via negative regulation of the Roundabout Axon Guidance Receptor Homolog 1 (Robo1) leading to activation of a Myc transcriptional programme.

Key words: Id proteins, Robo1, Cancer stem cell, Metastasis, Myc signature

Introduction

Several lines of evidence suggest that rare sub-populations of tumor cells, commonly termed cancer stem cells (CSCs), drive key tumor phenotypes such as self-renewal, drug resistance and metastasis and contribute to disease relapse and associated patient mortality (1-4). Recent evidence points to the hypothesis that CSCs are not static, but they exist in dynamic states, driven by critical transcription factors and are highly dependent on the microenvironmental cues (5-7). Understanding the molecular networks that are critical to the survival and plasticity of CSCs is fundamental to resolving clinical problems associated with chemo-resistance and metastatic residual disease.

The Inhibitor of DNA binding (ID) proteins have previously been recognized as regulators of CSCs and tumor progression (8). These proteins constitute a family of four highly conserved transcriptional regulators (ID1-4) that act as dominant-negative inhibitors of basic helix–loop–helix (bHLH) transcription factors. ID proteins are expressed in a tissue-specific and stage-dependent manner and are required for the maintenance of self-renewal and multipotency of embryonic and many tissue stem cells (9-12) . Previous studies have reported a functional redundancy among the four members of the mammalian Id family, in particular Id1 and Id3 (referred to collectively here as Id), and their overlapping expression patterns during normal development and cancer (13-17).

A number of studies have implied a significant role for ID1 and ID3 in breast cancer progression and metastasis (14). We have previously demonstrated that Id1 cooperates with activated Ras signalling and promotes mammary tumor initiation and metastasis *in vivo* by supporting long-term self-renewal and proliferative capacity (18). Additional work has clearly implicated ID1 in regulating D- and E-type cyclins and their associated cyclin-dependant kinases, CDK4 and CDK2 in human breast epithelial cells , p21 (19), the matrix

metalloproteinase MT1-MMP (20), KLF17 (21), Cyclin D1 (22), Bcl-2 (23), and BMI1 (24) among others.

Even though several Id-dependent targets have been identified, we still lack a comprehensive picture of the downstream molecular mechanisms controlled by Id and their associated pathways mediating breast cancer progression and metastasis particularly in the poor prognostic TNBC subtype. In this study**,** we demonstrate using three independent mouse models of TNBC that Id is important for the maintenance of a CSC phenotype. We also describe a novel mechanism by which Id controls the CSC state by negatively regulating Robo1 to control proliferation and self-renewal via activation of a Myc transcriptional programme.

Results

Id marks a subset of cells with stem-like properties in TNBC models

We investigated the role of Id in the context of CSC biology in the TNBC molecular subtype. Immunohistochemistry (IHC) analysis revealed that ID1 is expressed by a small minority of cells (range 0.5-6% of total cancer cells) in ~50 % of ER-negative disease, namely TNBC and Her2+ tumors (Supplementary Figure 1A, B). No significant difference in the distribution of ID3 expression was observed across different subtypes (data not shown).

To test the hypothesis that $Id1^+$ cells have a unique malignant phenotype, we developed two murine models of TNBC that permit the prospective isolation of $Id1^+$ cells for functional assays. In the first, we used the p53-/- TNBC tumor model where IHC analysis revealed that ~ 5% of neoplastic cells expressed Id1, consistent with the observation in the clinical samples, while Id3 marked a majority of the tumor cells in this model (Figure 1A).

To create a genetic reporter cell line, p53-/- mammary tumor cells were transduced with a lentiviral GFP reporter construct under the control of the Id1 promoter (Id1/GFP), as described previously (25) (Supplementary Figure 1C). FACS sorting for GFP expression followed by immunoblotting confirmed the ability of the Id1/GFP construct to prospectively enrich for Id1+ cells from this model (Supplementary Figure 1D). We next sought to understand if Id1 marked cells with high self-renewal capacity in this model using tumorsphere assays, a well-established surrogate for cells with high self-renewal capacity (26, 27). We observed an increase in the self-renewal capacity of $Id1/GFP^+$ cells when compared to the unsorted cell population in the p53-/- model (Figure 1B).

To establish the *in vivo* relevance of the increased self-renewal capacity of the $Id1/GFP^+$ tumor cells observed *in vitro*, we determined the tumor initiating capacity (TIC) of the $Id1/GFP^+$ cells using the limiting dilution assay (28). $Id1/GFP^+$ cells (1/42) showed more than a 7-fold increase in tumor initiating cell frequency over $Id1/GFP^-$ cells (1/314) after serial passage (Figure 1C).

We used the Id1C3-Tag tumor model as a second murine model to assess the phenotype of $Id1^+$ cells. In the C3-Tag tumor model, the expression of SV40-large T antigen in the mammary epithelium under the control of the C3 promoter leads to the development of TNBC in mice (29, 30). These tumors (C3-Tag) closely model the TNBC subtype as assessed by gene expression profiling (30). To generate a genetic reporter of Id1 promoter activity in TNBC, the C3-Tag model was crossed to a genetic reporter mouse model in which GFP is knocked into the intron 1 of the Id1 gene (31). The resulting Id1GFPC3-Tag mice (called Id1C3-Tag model) developed mammary tumors with similar kinetics as the parental C3-Tag mice and have a classical basal phenotype characterized by $CK14^+/CK8^-$ phenotype (Supplementary Figure 1E). 5% and 60% of cells in the Id1C3-Tag tumor were stained positive for Id1 and Id3 expression, respectively, as observed by IHC (Figure 1D). We were able to isolate $Id1^+$ tumor cells with a high degree of purity by FACS based on GFP expression followed by q-RT PCR (Figure 1E). The sorted cells were put into primary tumorsphere assay and the spheres were serially passaged to secondary and tertiary spheres which robustly selects for self-renewing cell populations. Similar to the p53-/- Id1/GFP model, $Id1^+/GFP^+$ cells from the Id1C3-Tag model were enriched for sphere-forming capacity (Figure 1F).

Using the Id1C3-Tag model, we also looked at the association of Id1/GFP expression with the expression of established CSC markers CD29, CD24 and CD61. $CD29^+/CD24^+$ status was previously reported to mark the tumorigenic subpopulation of cells in murine mammary tumors (32, 33). The $Id1^+/GFP^+$ cells in the Id1C3-Tag model are predominantly of the $CD29^+/CD24^+$ phenotype (Figure 1G), with a 1.6-fold higher proportion of cells expressing both CD29 and CD24 compared to the $Id1^-/GFP^-$ cells which comprise the bulk of the tumor. Interestingly, $Id1^+/GFP^+$ cells are also highly enriched for $CD24^+/CD61^+$ expression (more than 6-fold increase in $Id1^+/GFP^+$ cells), which was also reported to mark a murine breast CSC population (34) (Figure 1G).

We found no correlation between Id1 expression (as indicated by GFP^+) and the $CD29^+/CD24^+$ phenotype in the first transplantation round (T1) using the p53-/- model, as the percentage of $CD29^+/CD24^+$ cells was similar across each gating group (Supplementary Figure 1F). Interestingly, the $Id1^+$ cells, which are the putative cells that give rise to the increased TIC as shown in Figure 1C, showed 10 times less $CD24^+/CD29^+$ cells in the second transplantation round(T2) (34). The ability of the markers like CD24, CD29 and CD61 to identify the CSC population is clearly model-dependent. In addition to CD29 and CD24, the percentage of GFP^+ cells were also analysed and a higher percentage of GFP^+ cells was found in the second transplantation round of the p53-/- tumor compared to the first round tumor result (Supplementary Figure 1G), consistent with the increase in TICs reported in Figure 1C.

Id requirement for self-renewal *in vitro* and metastatic competency *in vivo*

We next assessed the requirement for Id1 and Id3 in maintaining the CSC phenotypes. Numerous studies have shown that there exists a functional redundancy between Id1 and Id3, so studies typically require depletion of both the factors to reveal a phenotype (35). We used the transplantable syngeneic 4T1 TNBC model, which has a high propensity to spontaneously metastasize to distant sites (including bone, lung, brain and liver), mimicking the aggressiveness of human breast cancers (36-41). IHC analysis showed that 15% of 4T1 tumor cells express high levels of Id1, and 35% have intermediate levels of Id1 expression, whereas the expression of Id3 was found in most of the cells (Figure 2A).

We used an inducible lentiviral shRNA system (42) that permits reversible knock down of Id1 and Id3 in response to doxycycline (Dox) treatment. Two clonal 4T1 cell lines, K1 and K2 were chosen along with a control line (C), based on the efficiency of Id knock down (Figure 2B, Supplementary Figure 2A). Id depletion resulted in a significant decrease in cell

proliferation and migration *in vitro* when compared to the control (Supplementary figure 2 B, C, D).

We next interrogated the effect of Id depletion on the self-renewal capacity of the C, K1 and K2 cell lines. Dox-dependent shRNA induction significantly reduced the ability of the K1 and K2 cells to form primary tumorspheres in the suspension culture (Figure 2C). This effect was not observed in the control cell line (C; Figure 2C). A significant further decrease in self-renewal capacity of K1 and K2 lines was observed when primary tumorspheres were passaged to the secondary stage (Figure 2D, E). The Id depleted tumorspheres were also markedly smaller in size compared to controls (Figure 2E, Supplementary Figure 2E).

To assess if the self-renewal phenotype controlled by Id is reversible, we firstly passaged primary tumorspheres [previously treated with Dox (K+)] to secondary tumorspheres. The secondary tumorspheres were then cultured in the presence or absence of Dox, to maintain the Id knockdown status or to allow the re-expression of Id, respectively (Supplementary Figure 2F, G). The secondary tumorspheres cultured without Dox (K1+-) re-established their self-renewal capacity as evidenced by the ability to form new tumorspheres (Figure 2F; Supplementary Figure 2H, I), suggesting that Id depletion does not lead to a permanent loss of self-renewal capacity.

To determine whether Id1 and Id3 are required for primary tumor and metastatic growth *in vivo*, K1 cells were orthotopically transplanted into the mammary fat pad of BALB/c mice. Dox-mediated knockdown of Id resulted in modest inhibition of primary tumor growth, with control tumors growing faster and reaching the ethical endpoint earlier than the Id knockdown group (Figure 2G). More significantly, mice transplanted with Id depleted K1 cells presented far fewer lung metastatic lesions compared to the control despite growing in the host for a longer time ($p<0.0001$; Figure 2H).

To assess the role for Id in metastatic progression *in vivo*, we examined Id expression in lung metastasis compared to primary tumors in mice injected with K1 cells. An increase in the expression of Id1 was observed in the lung metastasis in all the samples, while no significant enrichment of Id3 expression was observed (Supplementary Figure 3A). To determine whether altered expression patterns of ID1 are associated with metastasic progression in patients, ID1 IHC was performed on a cohort of 49 cases with matching primary tumor and brain metastatic lesions surgically removed from breast cancer patients. Amongst the 13 cases in which ID1 was detected by IHC in the primary tumor, an enrichment of ID1 expression was observed in brain metastases over the patient-matched primary tumor in 11 cases (Supplementary Figure 3B, Supplementary Table 1). Together with data from the animal model, this result suggests that ID1 promotes metastatic dissemination in a subset of human breast cancers.

Identification of genes and pathways regulated by Id

The canonical role for Id proteins is to regulate gene expression through association with transcription factors, yet a comprehensive analysis of Id transcriptional targets in cancer has not been reported. We performed gene expression profiling of Control (C) and Id depleted K1 cells. The gene expression profiles of four independent replicates (R1, R2, R3 and R4 ± doxycycline treatment) were compared by microarray analysis (Supplementary Figure 4A). 6081 differentially expressed genes were identified ($Q<0.05$), with 3310 up-regulated and 2771 down-regulated genes in Id KD cells (Supplementary Table 2 shows the top 25 differentially regulated genes). Network and pathway enrichment analysis was conducted using the MetaCore^{TM} software. 4301 significant network objects were identified for the Id knockdown microarray data (adjusted p-value of ≤ 0.05). The top pathways affected by Id knockdown were mostly associated with the cell cycle (Figure 3A, B) consistent with the loss of proliferative phenotype described previously (Supplementary Figure 2B, C). Similar results were obtained

using Gene Set Enrichment Analysis (GSEA) with significant down regulation of proliferative signatures (CELL_CYCLE_PROCESS) and mitosis (M_PHASE) (Supplementary Table 3). Genes such as CCNA2, CHEK1 and PLK1 in these gene sets are down-regulated by Id knockdown. This is consistent with our results (Supplementary figure 2 B, C) showing Id proteins are necessary for proliferation of 4T1 cells, as well as previous studies which reported a role of Id in controlling cell cycle progression and proliferation pathways (17, 43). Enrichment for genes involved in several oncogenic pathways such as Mek, Vegf, Myc and Bmi1 signalling have also been highlighted (Supplementary Table 4). In order to identify whether Id specifically regulate genes controlling breast cancer metastasis, GSEA analysis was performed with a collection of custom "metastasis gene sets". This collection (Table 1) consists of several metastatic signatures from the C2 collection (MSigDB database; Supplementary Table 5), combined with a list of custom gene sets described in major studies (44-53) as shown in Figure 3C. Genes differentially expressed in this set included *Robo1* (54, 55), *Il6* (56), *Fermt1* (57), *Foxc2* (58) and Mir30a (59). Three putative Id targets *Robo1*, *Fermt1* and *Mir30a* were then validated using q-RT PCR (Figure 3D) and found to be differentially regulated in the K1 cell line upon Id KD.

Id mediated inhibition of Robo1 controls the proliferative phenotype via activation of Myc transcription

Since Robo1 is known to have a tumor suppressor role in breast cancer biology (54, 60), we next sought to determine if Robo1 has an epistatic interaction with Id loss of function using siRNA mediated knockdown of Robo1 followed by proliferation assays. Knockdown of *Robo1* ameliorated the requirement for Id and rescued approximately 55 % of the proliferative decrease induced by Id KD (Figure 4A).

To understand the mechanisms by which *Robo1* increases the proliferative potential of Id depleted cells *in vitro*, we performed RNA-Sequencing (RNA-Seq) experiments on K1 cells with dox-inducible Id KD and/or Robo1 depletion using siRNA. Four replicates per condition were generated and MDS plots presented in Supplementary figure 4B showed that the replicates cluster together. Id KD alone in the K1 cells down regulated 4409 genes and up regulated 5236 genes (FDR<0.05), respectively. The majority of the differentially expressed genes determined by microarray were found by RNA-Seq analysis (Supplementary Figure 4C). Id depletion led to an increase in *Robo1* expression, as observed in the previous microarray experiment (Figure 3C, D; Figure 4 B).

Given that Id repressed Robo1 expression, we sought to determine Robo1 target genes in the absence of Id. Remarkably, under Id depletion conditions, *Robo1* KD restored expression of a large subset (~45%) of Id target genes to basal levels (Figure 4C). In comparison, knockdown of Id or Robo1 regulated few targets in the same direction (e.g. both up or both down). This implies that a large proportion of Id targets may be regulated via suppression of Robo1. Genes whose expression was repressed by Id KD and rescued by concomitant Robo1 KD were termed 'Intersect 1' (Figure 4C, Table 2). Genes that were upregulated by Id KD and downregulated by Robo1 KD (in the absence of Id) were annotated 'intersect 2' (Figure 4C, Table 3). To investigate the function of these intersect group of genes, we performed GSEA analysis using the MSigDB hallmark gene set (61). The top signatures in Intersect 1 were involved in cell proliferation, with enrichment for G2M checkpoint, E2F and Myc targets as well as mTOR signalling (Table 2). Rank-based analysis revealed strong negative enrichment for the hallmark Myc targets signature upon Id knockdown alone, and strong positive enrichment upon Id and Robo1 knockdown (Figure 4D). This suggests that following Id KD, Robo1 is induced and exerts anti-proliferative effects via suppression of Myc and its target genes (Supplementary Figure 4D, E). Transcription factor motif analysis using EnrichR revealed that Myc and its

binding partner Max, have a high combined score in the Intersect 1 gene list further implicating Myc as downstream effector of Robo1 and Id (Figure 4 E).

We were interested in investigating the possibility that Robo1 may exert its negative effects on the Myc pathway via regulation of Myc co-factors, which can potently enhance or suppress Myc transcriptional activity (62). In order to test this hypothesis, we looked at known Myc co-factors from the literature in our RNA-Seq data to determine if they were differentially expressed in the Id1 and Robo1 KD conditions. As seen in Supplementary Table 6, we included negative (red) and positive (green) cofactors in the analysis. Scrutiny of this list suggests that there are numerous negative co-factors (7/10) being induced and activators being repressed (13/24) by Robo1. For example, putative activation of the gene Rlim by Robo1. The encoded protein RLIM is an E3 ubiquitin ligase that suppresses the transcriptional activity of MYC (62).

In order to determine the interaction between ID and ROBO1 in human TNBCs, 82 publicly available TNBC datasets from The Cancer Genome Atlas [TCGA, (63)] were queried for the mRNA expressions of ID1, ID3, and ROBO1 and the expression heats maps were generated using cBioportal (64, 65). Consistent with our results, a trend towards negative interaction between ID and ROBO1 was observed (correlation coefficient -0.09) (Supplementary Figure 4F, G).

In summary, we have demonstrated that Id depletion leads to a loss in the proliferative and self-renewal cancer stem cell phenotypes associated with TNBC. Id1 acts by negatively regulating Robo1 which in turn leads to the activation of a Myc transcriptional program (Figure 5).

Discussion

There is increasing evidence that all cells within a tumor are not equal with some cells having the plasticity to adapt and subvert cellular and molecular mechanisms to be more tumorigenic than others. In this study, we demonstrate that Id1 and its closely related family member Id3 are important for the CSC phenotype in the TNBC subtype. Using three independent models of Id expression and depletion, we demonstrate that the properties of proliferation and self-renewal are regulated by Id proteins.

Transcription factors like the Id family of proteins can affect a number of key molecular pathways, allowing switching of phenotypes in response to local cues such as transforming growth factor-β (TGF-β) (12, 66), receptor tyrosine kinase signalling (67), and steroid hormones (68) and therefore are able to transduce a multitude of cues into competency for proliferation and self-renewal. The CSC phenotype as marked by Id is plastic, fitting with the latest evidence that CSC are not necessarily hierarchically organised, but rather represent a transient inducible state dependent on the local microenvironment.

We report the first comprehensive analysis of Id transcriptional targets. We go on to identify a novel epistatic relationship with Robo1, with Robo1 loss sufficient to remove the necessity for Id in proliferation, suggesting that suppression of Robo1 is an important function for Id in this setting. Robo1 is a receptor for SLIT1 and SLIT2 that mediates cellular responses to molecular guidance cues in cellular migration (69). Previous work with mammary stem cells showed that the extracellular SLIT2 signals via ROBO1 to regulate the asymmetric self-renewal of basal stem cells through the transcription factor Snail during mammary gland development (70). Our finding may have significant implications for tumor biology because SLIT/ROBO signalling is altered in about 40% of basal breast tumors (70). Our work implicates a novel role for SLIT-

ROBO signalling in CSC and shows a new mechanism by which Id proteins control the self-renewal phenotype by suppressing the Robo1 tumor suppressor role in TNBC.

The significant decrease in the Myc levels on Id knockdown suggest an Id/ Robo1/ Myc axis in TNBC (Supplementary Figure 4D, E). While the proposed model for regulation of Myc is not quite clear, we propose two possible modes of regulation of Myc: (1) Robo independent suppression of Myc expression and (2) Robo dependent regulation of Myc activity. Though the mechanism still needs to be elaborated, we hypothesise that in the absence of Id, Robo1 inhibits Myc activity via activation of Myc inhibitors (e.g. Rlim) and/or inhibition of Myc activators (e.g. Aurka). This is borne out by the analysis of Myc co-factors in the Id and Id Robo1 KD RNA Seq data (Supplementary table 6). Further work is needed to determine whether, and which, Myc cofactors are epistatic to Id-Robo1 signalling. Our data provides further evidence that Robo1 is an important suppressor of proliferation and self-renewal in TNBC. Prior work showing high Robo1 expression association with good outcome in breast cancer is consistent with our finding (54). There has been substantial interest in targeting Myc (60, 71) and Id1, but until now has been very challenging (20, 72). We show that Id1 is able to reprogram Myc activity via Robo1 and may provide an alternative strategy to target Myc-dependent transcription.

Material and Methods

Lentivirus production

Lentiviral supernatant was produced by transfecting each lentiviral expression vector along with third-generation lentiviral packaging and pseudotyping plasmids (73) into the packaging cell line HEK293T. Briefly, 1.4 x 10^6 cells were seeded in a 60mm tissue culture dish and grown to 80% confluence. 3µg of expression plasmid was co-transfected with lentiviral packaging and pseudotyping plasmids (2.25µg each of pMDLg/pRRE and pRSV-REV and 1.5µg of pMD2.G), using Lipofectamine 2000 (Invitrogen, Mulgrave, Vic, Australia) according to the manufacturer's protocol. Cell culture medium was replaced after 24hr. The viral supernatant was collected 48hr post transfection and filtered using a 0.45µm filter. The filtered lentiviral supernatant was concentrated 20-fold by using Amicon Ultra-4 filter units (100 kDa NMWL) (Millipore, North Ryde, NSW, Australia).

Lentiviral infection

4T1 cells were plated at a density of 1.0 x 10^5 cells per well in 6-well tissue culture plates and culture medium was replaced after 24hr with medium containing 8µg/mL of polybrene (Sigma-Aldrich, Lismore, NSW, Australia). The cells were infected overnight with the concentrated virus at 1:5 dilution. Culture medium was changed 24hr post infection and cells were grown until reaching confluence. Cells transduced with both pSLIK-Venus-TmiR-Id1 and pSLIK-Neo-TmiR-Id3 were sorted on FACS using Venus as a marker followed by selection with neomycin at 400µg/mL for 5 days. Cells transduced with pSLIK-Neo-TmiR-EGFP were also selected with neomycin.

Tumorsphere assay

Cells dissociated from modified 4T1 cells and p53-/- Id1/GFP, Id1C3-Tag tumors were put into tumorsphere assay as described previously (28)**.**

Limiting dilution assay

Single-cell suspensions of FACS sorted Id1/GFP+ or unsorted viable tumor cells were prepared as described previously. Tumor cells were transplanted in appropriate numbers into the fourth mammary fat pad of 8- to 12-week-old FVB/N mice and aged till ethical end point. Extreme limiting dilution analysis71 software was used to calculate the TPF.

Microarray and bioinformatics analysis

Total RNA from the samples were isolated using Qiagen RNeasy minikit (Qiagen, Doncaster, VIC, Australia. cDNA synthesis, probe labelling, hybridization, scanning and data processing were all conducted by the Ramaciotti Centre for Gene Function Analysis (The University of New South Wales). Gene expression profiling was performed using the Affymetrix GeneChip® Mouse Gene 2.0 ST Array. Normalization and probe-set summarization was performed using the robust multichip average method (74) implemented in the Affymetrix Power Tools apt-probeset-summarize software (version 1.15.0) (using the -a rma option). Differential expression between experimental groups was assessed using Limma (75) via the limmaGP tool in GenePattern (76). Gene Set Enrichment Analysis (GSEA) (http://www.broadinstitute.org/gsea) (77) was performed using the GSEA Pre-ranked module on a ranked list of the limma moderated t-statistics, against gene-sets from v4.0 of the MSigDB (77) and custom gene-sets derived from the literature. Microarray data are freely available from GEO: GSE129790

Next generation sequencing

$3.5x10^4$ 4T1 K1 cells were seeded in 6-well plates in 4T1 media and treated with or without Doxorubicin (1 µg/mL) to induce Id1/3 knockdown. Cells were also transfected with non-targeting control siRNA (Dharmacon D-001810-10-05) or Robo1 siRNA (Dharmacon M-046944-01-0010). Cells were harvested after 48 hours and total RNA was extracted using the automated QiaSymphony magnetic bead extraction system. The Illumina TruSeq Stranded mRNA Library Prep Kit was used to generate libraries with 1 µg of input RNA following the manufacturer's instructions. cDNA libraries were sequenced on the NextSeq system (Illumina), with 75 bp paired-end reads. Quality control was checked using FastQC (bioinformatics.babraham.ac.uk/projects/fastqc). Reads were then aligned to the mouse reference genome Mm10 using STAR ultrafast universal RNA-Seq aligner (78). Gene feature counting was performed with RSEM (79). Replicate 3 from the Id1 KD group showed no KD of Id1 by qPCR and was therefore removed prior to down-stream differential expression analysis. Transcripts with expression counts of 0 across all samples were removed and then normalised using TMM (80). The normalized counts were then log transformed using voom (81) and differential expression was performed with limma (75). Differentially expressed genes were visualized and explored using Degust (http://degust.erc.monash.edu/). Genes with false discovery rate (FDR)<0.05 were considered significantly differentially expressed. For GSEA analysis, genes were ranked based on the limma moderated t-statistic and this was used as input for the GSEA desktop application (77). RNA sequencing data are freely available from GEO: GSE129858.

Microarray (GSE129790) and RNA-Seq (GSE129858) datasets are available in SuperSeries GSE129859.

Statistical analysis

Statistical analyses were performed using GraphPad Prism 6. All *in vitro* experiments were done in 3 biological replicates each with 2 or more technical replicates. 5-10 mice were used per condition for the *in vivo* experiments. Data represented are means ± standard deviation. Statistical tests used are Unpaired student t-test and two-way-ANOVA. p-values <0.05 were considered statistically significant with *$p< 0.05$, **$p< 0.01$, *** $p< 0.001$, **** $p< 0.0001$.

Acknowledgements

We would like to thank the following people for their assistance with this manuscript: Ms. Nicola Foreman and Ms. Breanna Fitzpatrick for animal handling; Ms. Alice Boulghourjian and Ms. Anaiis Zaratzian for tissue processing and IHC staining; Mr. Rob Salomon and Mr. David Snowden for their help with flow sorting.

This work was supported by funding from the National Health and Medical Research Council (NHMRC) of Australia, The National Breast Cancer Foundation and John and Deborah McMurtrie and in part by Early Career Research (ECR) Award from Science and Engineering Research Board (SERB), Government of India (ECR/2015/000031). A.S. is the recipient of a Senior Research Fellowship from the NHMRC. S.O.T. is supported by NBCF practitioner fellowship and also acknowledges the Sydney Breast Cancer Foundation, the Tag family, Mr David Paradice, ICAP and the O'Sullivan family and the estate of the late Kylie Sinclair. RN is the recipient of the Ramanujan Fellowship from the Government of India (SERB) (SB/S2/RJN/182/2014). WST is funded by International Postgraduate Research Scholarship and the Beth Yarrow Memorial Award in Medical Science. APT and BAV is funded through CSIR- Junior Research Fellowship, and DST- INSPIRE Fellowship, respectively.

Competing interests

The authors declare no conflict of interest.

References

1. Chen J, Li Y, Yu TS, McKay RM, Burns DK, Kernie SG, et al. A restricted cell population propagates glioblastoma growth after chemotherapy. Nature. 2012;488(7412):522-6.
2. Lawson DA, Bhakta NR, Kessenbrock K, Prummel KD, Yu Y, Takai K, et al. Single-cell analysis reveals a stem-cell program in human metastatic breast cancer cells. Nature. 2015;526(7571):131-5.
3. Li X, Lewis MT, Huang J, Gutierrez C, Osborne CK, Wu MF, et al. Intrinsic resistance of tumorigenic breast cancer cells to chemotherapy. J Natl Cancer Inst. 2008;100(9):672-9.
4. Malanchi I, Santamaria-Martinez A, Susanto E, Peng H, Lehr HA, Delaloye JF, et al. Interactions between cancer stem cells and their niche govern metastatic colonization. Nature. 2011;481(7379):85-9.
5. da Silva-Diz V, Lorenzo-Sanz L, Bernat-Peguera A, Lopez-Cerda M, Munoz P. Cancer cell plasticity: Impact on tumor progression and therapy response. Seminars in cancer biology. 2018.
6. Lee G, Hall RR, 3rd, Ahmed AU. Cancer Stem Cells: Cellular Plasticity, Niche, and its Clinical Relevance. J Stem Cell Res Ther. 2016;6(10).
7. Wahl GM, Spike BT. Cell state plasticity, stem cells, EMT, and the generation of intra-tumoral heterogeneity. NPJ Breast Cancer. 2017;3:14.
8. Lasorella A, Benezra R, Iavarone A. The ID proteins: master regulators of cancer stem cells and tumour aggressiveness. Nature reviews Cancer. 2014;14(2):77-91.
9. Aloia L, Gutierrez A, Caballero JM, Di Croce L. Direct interaction between Id1 and Zrf1 controls neural differentiation of embryonic stem cells. EMBO Rep. 2015;16(1):63-70.
10. Hong SH, Lee JH, Lee JB, Ji J, Bhatia M. ID1 and ID3 represent conserved negative regulators of human embryonic and induced pluripotent stem cell hematopoiesis. J Cell Sci. 2011;124(Pt 9):1445-52.
11. Liang YY, Brunicardi FC, Lin X. Smad3 mediates immediate early induction of Id1 by TGF-beta. Cell Res. 2009;19(1):140-8.
12. Stankic M, Pavlovic S, Chin Y, Brogi E, Padua D, Norton L, et al. TGF-beta-Id1 signaling opposes Twist1 and promotes metastatic colonization via a mesenchymal-to-epithelial transition. Cell reports. 2013;5(5):1228-42.
13. Anido J, Saez-Borderias A, Gonzalez-Junca A, Rodon L, Folch G, Carmona MA, et al. TGF-beta Receptor Inhibitors Target the CD44(high)/Id1(high) Glioma-Initiating Cell Population in Human Glioblastoma. Cancer cell. 2010;18(6):655-68.
14. Gupta GP, Perk J, Acharyya S, de Candia P, Mittal V, Todorova-Manova K, et al. ID genes mediate tumor reinitiation during breast cancer lung metastasis. Proceedings of the National Academy of Sciences of the United States of America. 2007;104(49):19506-11.
15. Lyden D, Young AZ, Zagzag D, Yan W, Gerald W, O'Reilly R, et al. Id1 and Id3 are required for neurogenesis, angiogenesis and vascularization of tumour xenografts. Nature. 1999;401(6754):670-7.
16. Niola F, Zhao X, Singh D, Sullivan R, Castano A, Verrico A, et al. Mesenchymal high-grade glioma is maintained by the ID-RAP1 axis. The Journal of clinical investigation. 2013;123(1):405-17.
17. O'Brien CA, Kreso A, Ryan P, Hermans KG, Gibson L, Wang Y, et al. ID1 and ID3 regulate the self-renewal capacity of human colon cancer-initiating cells through p21. Cancer cell. 2012;21(6):777-92.
18. Swarbrick A, Roy E, Allen T, Bishop JM. Id1 cooperates with oncogenic Ras to induce metastatic mammary carcinoma by subversion of the cellular senescence response. Proceedings of the National Academy of Sciences of the United States of America. 2008;105(14):5402-7.
19. Swarbrick A, Akerfeldt MC, Lee CS, Sergio CM, Caldon CE, Hunter LJ, et al. Regulation of cyclin expression and cell cycle progression in breast epithelial cells by the helix-loop-helix protein Id1. Oncogene. 2005;24(3):381-9.
20. Fong S, Itahana Y, Sumida T, Singh J, Coppe JP, Liu Y, et al. Id-1 as a molecular target in therapy for breast cancer cell invasion and metastasis. Proceedings of the National Academy of Sciences of the United States of America. 2003;100(23):13543-8.

21. Gumireddy K, Li A, Gimotty PA, Klein-Szanto AJ, Showe LC, Katsaros D, et al. KLF17 is a negative regulator of epithelial-mesenchymal transition and metastasis in breast cancer. Nat Cell Biol. 2009;11(11):1297-304.
22. Tobin NP, Sims AH, Lundgren KL, Lehn S, Landberg G. Cyclin D1, Id1 and EMT in breast cancer. BMC cancer. 2011;11:417.
23. Kim H, Chung H, Kim HJ, Lee JY, Oh MY, Kim Y, et al. Id-1 regulates Bcl-2 and Bax expression through p53 and NF-kappaB in MCF-7 breast cancer cells. Breast Cancer Res Treat. 2008;112(2):287-96.
24. Qian T, Lee JY, Park JH, Kim HJ, Kong G. Id1 enhances RING1b E3 ubiquitin ligase activity through the Mel-18/Bmi-1 polycomb group complex. Oncogene. 2010;29(43):5818-27.
25. Mellick AS, Plummer PN, Nolan DJ, Gao D, Bambino K, Hahn M, et al. Using the transcription factor inhibitor of DNA binding 1 to selectively target endothelial progenitor cells offers novel strategies to inhibit tumor angiogenesis and growth. Cancer research. 2010;70(18):7273-82.
26. Lee CH, Yu CC, Wang BY, Chang WW. Tumorsphere as an effective in vitro platform for screening anti-cancer stem cell drugs. Oncotarget. 2016;7(2):1215-26.
27. Pastrana E, Silva-Vargas V, Doetsch F. Eyes wide open: a critical review of sphere-formation as an assay for stem cells. Cell Stem Cell. 2011;8(5):486-98.
28. Nair R, Roden DL, Teo WS, McFarland A, Junankar S, Ye S, et al. c-Myc and Her2 cooperate to drive a stem-like phenotype with poor prognosis in breast cancer. Oncogene. 2014;33(30):3992-4002.
29. Green JE, Shibata MA, Yoshidome K, Liu ML, Jorcyk C, Anver MR, et al. The C3(1)/SV40 T-antigen transgenic mouse model of mammary cancer: ductal epithelial cell targeting with multistage progression to carcinoma. Oncogene. 2000;19(8):1020-7.
30. Pfefferle AD, Herschkowitz JI, Usary J, Harrell JC, Spike BT, Adams JR, et al. Transcriptomic classification of genetically engineered mouse models of breast cancer identifies human subtype counterparts. Genome biology. 2013;14(11):R125.
31. Perry SS, Zhao Y, Nie L, Cochrane SW, Huang Z, Sun XH. Id1, but not Id3, directs long-term repopulating hematopoietic stem-cell maintenance. Blood. 2007;110(7):2351-60.
32. Herschkowitz JI, Zhao W, Zhang M, Usary J, Murrow G, Edwards D, et al. Comparative oncogenomics identifies breast tumors enriched in functional tumor-initiating cells. Proceedings of the National Academy of Sciences of the United States of America. 2012;109(8):2778-83.
33. Zhang M, Behbod F, Atkinson RL, Landis MD, Kittrell F, Edwards D, et al. Identification of tumor-initiating cells in a p53-null mouse model of breast cancer. Cancer research. 2008;68(12):4674-82.
34. Vaillant F, Asselin-Labat ML, Shackleton M, Forrest NC, Lindeman GJ, Visvader JE. The mammary progenitor marker CD61/beta3 integrin identifies cancer stem cells in mouse models of mammary tumorigenesis. Cancer research. 2008;68(19):7711-7.
35. Konrad CV, Murali R, Varghese BA, Nair R. The role of cancer stem cells in tumor heterogeneity and resistance to therapy. Can J Physiol Pharmacol. 2017;95(1):1-15.
36. Yoneda T, Michigami T, Yi B, Williams PJ, Niewolna M, Hiraga T. Actions of bisphosphonate on bone metastasis in animal models of breast carcinoma. Cancer. 2000;88(12 Suppl):2979-88.
37. Lelekakis M, Moseley JM, Martin TJ, Hards D, Williams E, Ho P, et al. A novel orthotopic model of breast cancer metastasis to bone. Clin Exp Metastasis. 1999;17(2):163-70.
38. Tao K, Fang M, Alroy J, Sahagian GG. Imagable 4T1 model for the study of late stage breast cancer. BMC cancer. 2008;8:228.
39. Aslakson CJ, Miller FR. Selective events in the metastatic process defined by analysis of the sequential dissemination of subpopulations of a mouse mammary tumor. Cancer research. 1992;52(6):1399-405.
40. Pulaski BA, Ostrand-Rosenberg S. Reduction of established spontaneous mammary carcinoma metastases following immunotherapy with major histocompatibility complex class II and B7.1 cell-based tumor vaccines. Cancer research. 1998;58(7):1486-93.
41. Eckhardt BL, Parker BS, van Laar RK, Restall CM, Natoli AL, Tavaria MD, et al. Genomic analysis of a spontaneous model of breast cancer metastasis to bone reveals a role for the extracellular matrix. Mol Cancer Res. 2005;3(1):1-13.

42. Shin KJ, Wall EA, Zavzavadjian JR, Santat LA, Liu J, Hwang JI, et al. A single lentiviral vector platform for microRNA-based conditional RNA interference and coordinated transgene expression. Proceedings of the National Academy of Sciences of the United States of America. 2006;103(37):13759-64.
43. Nair R, Teo WS, Mittal V, Swarbrick A. ID proteins regulate diverse aspects of cancer progression and provide novel therapeutic opportunities. Molecular therapy : the journal of the American Society of Gene Therapy. 2014;22(8):1407-15.
44. Aceto N, Bardia A, Miyamoto DT, Donaldson MC, Wittner BS, Spencer JA, et al. Circulating tumor cell clusters are oligoclonal precursors of breast cancer metastasis. Cell. 2014;158(5):1110-22.
45. Bos PD, Zhang XH, Nadal C, Shu W, Gomis RR, Nguyen DX, et al. Genes that mediate breast cancer metastasis to the brain. Nature. 2009;459(7249):1005-9.
46. Charafe-Jauffret E, Ginestier C, Iovino F, Wicinski J, Cervera N, Finetti P, et al. Breast cancer cell lines contain functional cancer stem cells with metastatic capacity and a distinct molecular signature. Cancer research. 2009;69(4):1302-13.
47. Dontu G, Al-Hajj M, Abdallah WM, Clarke MF, Wicha MS. Stem cells in normal breast development and breast cancer. Cell proliferation. 2003;36 Suppl 1:59-72.
48. Kang Y, Siegel PM, Shu W, Drobnjak M, Kakonen SM, Cordon-Cardo C, et al. A multigenic program mediating breast cancer metastasis to bone. Cancer cell. 2003;3(6):537-49.
49. Liu H, Patel MR, Prescher JA, Patsialou A, Qian D, Lin J, et al. Cancer stem cells from human breast tumors are involved in spontaneous metastases in orthotopic mouse models. Proceedings of the National Academy of Sciences of the United States of America. 2010;107(42):18115-20.
50. Minn AJ, Gupta GP, Siegel PM, Bos PD, Shu W, Giri DD, et al. Genes that mediate breast cancer metastasis to lung. Nature. 2005;436(7050):518-24.
51. Minn AJ, Kang Y, Serganova I, Gupta GP, Giri DD, Doubrovin M, et al. Distinct organ-specific metastatic potential of individual breast cancer cells and primary tumors. The Journal of clinical investigation. 2005;115(1):44-55.
52. Padua D, Zhang XH, Wang Q, Nadal C, Gerald WL, Gomis RR, et al. TGFbeta primes breast tumors for lung metastasis seeding through angiopoietin-like 4. Cell. 2008;133(1):66-77.
53. Tang B, Yoo N, Vu M, Mamura M, Nam JS, Ooshima A, et al. Transforming growth factor-beta can suppress tumorigenesis through effects on the putative cancer stem or early progenitor cell and committed progeny in a breast cancer xenograft model. Cancer research. 2007;67(18):8643-52.
54. Chang PH, Hwang-Verslues WW, Chang YC, Chen CC, Hsiao M, Jeng YM, et al. Activation of Robo1 signaling of breast cancer cells by Slit2 from stromal fibroblast restrains tumorigenesis via blocking PI3K/Akt/beta-catenin pathway. Cancer research. 2012;72(18):4652-61.
55. Qin F, Zhang H, Ma L, Liu X, Dai K, Li W, et al. Low Expression of Slit2 and Robo1 is Associated with Poor Prognosis and Brain-specific Metastasis of Breast Cancer Patients. Scientific reports. 2015;5:14430.
56. Chang Q, Bournazou E, Sansone P, Berishaj M, Gao SP, Daly L, et al. The IL-6/JAK/Stat3 feed-forward loop drives tumorigenesis and metastasis. Neoplasia. 2013;15(7):848-62.
57. Landemaine T, Jackson A, Bellahcene A, Rucci N, Sin S, Abad BM, et al. A six-gene signature predicting breast cancer lung metastasis. Cancer research. 2008;68(15):6092-9.
58. Mani SA, Yang J, Brooks M, Schwaninger G, Zhou A, Miura N, et al. Mesenchyme Forkhead 1 (FOXC2) plays a key role in metastasis and is associated with aggressive basal-like breast cancers. Proceedings of the National Academy of Sciences of the United States of America. 2007;104(24):10069-74.
59. Zhang N, Wang X, Huo Q, Sun M, Cai C, Liu Z, et al. MicroRNA-30a suppresses breast tumor growth and metastasis by targeting metadherin. Oncogene. 2014;33(24):3119-28.
60. Shen L, O'Shea JM, Kaadige MR, Cunha S, Wilde BR, Cohen AL, et al. Metabolic reprogramming in triple-negative breast cancer through Myc suppression of TXNIP. Proceedings of the National Academy of Sciences of the United States of America. 2015;112(17):5425-30.
61. Liberzon A, Birger C, Thorvaldsdottir H, Ghandi M, Mesirov JP, Tamayo P. The Molecular Signatures Database (MSigDB) hallmark gene set collection. Cell systems. 2015;1(6):417-25.
62. Gao R, Wang L, Cai H, Zhu J, Yu L. E3 Ubiquitin Ligase RLIM Negatively Regulates c-Myc Transcriptional Activity and Restrains Cell Proliferation. PloS one. 2016;11(9):e0164086.

63. Cancer Genome Atlas Research N, Weinstein JN, Collisson EA, Mills GB, Shaw KR, Ozenberger BA, et al. The Cancer Genome Atlas Pan-Cancer analysis project. Nature genetics. 2013;45(10):1113-20.
64. Gao J, Aksoy BA, Dogrusoz U, Dresdner G, Gross B, Sumer SO, et al. Integrative analysis of complex cancer genomics and clinical profiles using the cBioPortal. Science signaling. 2013;6(269):pl1.
65. Cerami E, Gao J, Dogrusoz U, Gross BE, Sumer SO, Aksoy BA, et al. The cBio cancer genomics portal: an open platform for exploring multidimensional cancer genomics data. Cancer discovery. 2012;2(5):401-4.
66. Kang Y, Chen CR, Massague J. A self-enabling TGFbeta response coupled to stress signaling: Smad engages stress response factor ATF3 for Id1 repression in epithelial cells. Molecular cell. 2003;11(4):915-26.
67. Tam WF, Gu TL, Chen J, Lee BH, Bullinger L, Frohling S, et al. Id1 is a common downstream target of oncogenic tyrosine kinases in leukemic cells. Blood. 2008;112(5):1981-92.
68. Lin CQ, Singh J, Murata K, Itahana Y, Parrinello S, Liang SH, et al. A role for Id-1 in the aggressive phenotype and steroid hormone response of human breast cancer cells. Cancer research. 2000;60(5):1332-40.
69. Huang T, Kang W, Cheng AS, Yu J, To KF. The emerging role of Slit-Robo pathway in gastric and other gastro intestinal cancers. BMC cancer. 2015;15:950.
70. Ballard MS, Zhu A, Iwai N, Stensrud M, Mapps A, Postiglione MP, et al. Mammary Stem Cell Self-Renewal Is Regulated by Slit2/Robo1 Signaling through SNAI1 and mINSC. Cell reports. 2015;13(2):290-301.
71. Yang A, Qin S, Schulte BA, Ethier SP, Tew KD, Wang GY. MYC Inhibition Depletes Cancer Stem-like Cells in Triple-Negative Breast Cancer. Cancer research. 2017;77(23):6641-50.
72. Dang CV, Reddy EP, Shokat KM, Soucek L. Drugging the 'undruggable' cancer targets. Nature reviews Cancer. 2017;17(8):502-8.
73. Dull T, Zufferey R, Kelly M, Mandel RJ, Nguyen M, Trono D, et al. A third-generation lentivirus vector with a conditional packaging system. Journal of virology. 1998;72(11):8463-71.
74. Irizarry RA, Bolstad BM, Collin F, Cope LM, Hobbs B, Speed TP. Summaries of Affymetrix GeneChip probe level data. Nucleic acids research. 2003;31(4):e15.
75. Smyth GK. Linear models and empirical bayes methods for assessing differential expression in microarray experiments. Statistical applications in genetics and molecular biology. 2004;3:Article3.
76. Reich M, Liefeld T, Gould J, Lerner J, Tamayo P, Mesirov JP. GenePattern 2.0. Nature genetics. 2006;38(5):500-1.
77. Subramanian A, Tamayo P, Mootha VK, Mukherjee S, Ebert BL, Gillette MA, et al. Gene set enrichment analysis: a knowledge-based approach for interpreting genome-wide expression profiles. Proceedings of the National Academy of Sciences of the United States of America. 2005;102(43):15545-50.
78. Dobin A, Davis CA, Schlesinger F, Drenkow J, Zaleski C, Jha S, et al. STAR: ultrafast universal RNA-seq aligner. Bioinformatics. 2013;29(1):15-21.
79. Li B, Dewey CN. RSEM: accurate transcript quantification from RNA-Seq data with or without a reference genome. BMC bioinformatics. 2011;12:323.
80. Robinson MD, Oshlack A. A scaling normalization method for differential expression analysis of RNA-seq data. Genome biology. 2010;11(3):R25.
81. Ritchie ME, Phipson B, Wu D, Hu Y, Law CW, Shi W, et al. limma powers differential expression analyses for RNA-sequencing and microarray studies. Nucleic acids research. 2015;43(7):e47.

Figure legends

Figure 1. Id1 marks tumor cells with high self-renewal in murine models of TNBC.

A. Representative IHC images of Id1 and Id3 expression in p53-/- tumor model. Black arrows in the inset indicate Id1+ cells. Scale bars = 50 μ m. **B.** p53-/- tumor cells were transfected with the Id1/GFP reporter and subsequently sorted for GFP expression. The self-renewal capacity of Id1/GFP$^+$ p53-/- cells was significantly higher than unsorted Id1/GFP p53-/- cells upon passage to tertiary tumorspheres. Data are means ± SD (n=3). (*** $p< 0.001$; Two-way ANOVA). **C.** Id1 expressing cells were sorted from the p53-/- Id1/GFP tumor model and transplanted into recipient mice by limiting dilution assay. Based on limiting dilution calculations (ELDA), the Id1$^+$ cells demonstrated a 7-fold enrichment in tumor initiating capacity (TIC) when compared to the Id1$^-$ cells in serial passage. **D.** Representative IHC images of the Id1C3-Tag model, confirming its suitability as a model system. Black arrows in the inset indicate Id1+ cells. Expression of Id1 was less than 5% as determined by IHC. Bars = 50 μ m. **E.** Tumor cells from the Id1C3-Tag tumor model were FACS sorted based on their GFP expression. qRT-PCR analyses on the sorted GFP$^+$ and GFP$^-$ cell populations showed a significant increase (more than 5-fold) for Id1 expression in the GFP$^+$ cells compared to cells lacking GFP expression. **F.** *In vitro* self-renewal capacity of GFP$^+$ cells was measured using the tumorsphere assay. The secondary sphere forming capacity of Id1$^+$ tumor cells from the Id1C3-Tag model was significantly enriched in comparison to the Id1$^-$tumor cells. Data are means ± SD (n=3). (**$p< 0.01$, **** $p< 0.0001$; Two-way ANOVA). **G.** Representative FACS scatterplot and histograms from Id1C3-Tag tumors showing the expression of the CSC markers CD24, CD29 and CD61 in the Id1$^-$/GFP$^-$ and Id1$^+$/GFP$^+$ cancer cells. Putative CSC populations are highlighted within the red box.

Figure 2. **Depletion of Id1 and Id3 leads to a reduced self-renewal capacity *in vitro* and metastatic potential *in vivo*. A.** Endogenous levels of Id1 and Id3 expression in 4T1primary mammary tumors were determined. 4T1 were cells stained for Id1 and Id3 expression (brown) and counterstained with haematoxylin. Mammary gland tissue from Id1 and Id3 null (Id1-/- and Id3-/-) mice served as negative controls. Scale bars = 50 μm. Western blot analysis of protein lysate from 4T1 tumor cells served as positive controls for Id1 and Id3 expression. **B.** Kinetics of conditional Id knockdown in 4T1 cells. Representative Western blot analysis of Id protein levels in pSLIK K1 cells over time. Cells were cultured in the presence of 1 μg/ml of Doxycycline (Dox) for 1, 3 and 5 days. β-actin was used as loading control. **C.** 4T1 Control, pSLIK K1 and K2 clones were assayed for their tumorsphere forming potential. Dox was added into the culture medium at day 0. Number of primary tumorspheres formed was quantified by visual examination on day 7. Id knockdown leads to a decrease in tumorsphere-forming ability of K1 and K2 cell lines. Data are means ± SD (n=3). (**$p< 0.01$; Two-way ANOVA). **D.** Primary tumorspheres were passaged and the number of secondary tumorspheres was quantified on day 14. Knockdown of Id significantly reduces the ability of the K1 and K2 cells to form secondary tumorspheres in the suspension culture. Data are means ± SD (n=3). (**$p< 0.01$; Two-way ANOVA). **E.** Representative images of primary and secondary tumorsphere formation for the clone K1 ±Dox. **F.** Quantification and representative images of primary tumorsphere treated with Dox (K1+) passaged to secondary spheres in Dox free conditions (K1+-) allowing re expression of Id and restoration of self-renewal capacity. **G.** Knockdown of Id significantly delays tumor growth in the 4T1 syngeneic model. (n = 10 mice; **p value<0.01, Student's t-test). **H.** Id knockdown suppresses spontaneous lung metastasis. Tumors depleted of Id expression generated fewer spontaneous lung macrometastatic lesions compared to the control despite growing in the host for a longer time. Inset shows

representative images of lungs bearing the control (K1 - Dox) and Id KD (K1 + Dox) lung metastases at ethical end point. Control; n = 8 mice, Id KD; n=10 mice. Scale bar = 50 um.

Figure 3. Gene expression analysis reveals targets of Id in TNBC

A, B. To characterize the network of genes regulated by Id, functional annotation analyses were performed on the gene array data from the 4T1 TNBC model. The Id depletion model attempted to identify downstream targets of Id through a loss of function approach. The gene expression profile of four independent replicates of the K1 shId clone, with and without doxycycline treatment, was compared by microarray analysis. This resulted in a list of differentially expressed genes between control and Id depleted cells, which by further network and map analysis using Metacore demonstrated was largely driven by genes controlling cell cycle pathways.

C. Gene expression analysis identified metastasis-related genes that were differentially expressed in response to Id knockdown. To determine if genes that mediate metastasis were enriched in the Id signature, gene expression analysis was performed using a manually curated set of metastasis gene sets. Genes differentially expressed in response to Id knockdown as well as associated with pathways regulating metastasis were identified based on reports from the literature which included Robo1.

D. Validation of expression profiling results by quantitative real-time-PCR using the Taqman® probe based system. Relative mRNA expression of Robo1, Fermt1 and Mir30a, in the 4T1 pSLIK shId Clonal cell line (K1) and pSLIK control (C), as indicated. Data are means ± SD (n=3). (**$p< 0.01$, **** $p< 0.0001$; unpaired t-test).

Figure 4. Identification of Myc signature activation by Id via negative regulation of Robo1

A. Proliferation of K1 cells treated with non-targeting (NT) control siRNA or Robo1 siRNA in the absence or presence of Doxycycline to induce Id knockdown was measured by the IncuCyte™ (Essen Instruments) live-cell imaging system. Data shown as mean ±SD (n=3). (*** $p< 0.001$; Unpaired two-tailed t-test). **B**. Robo1 expression in Control, Id KD, Robo1 KD and Id Robo1 KD cells was measured by quantitative PCR. Ct values were normalised to β actin and GAPDH housekeeping genes. Data shown as mean ± SEM (n=4). (** $p< 0.01$, **** $p < 0.0001$; Unpaired two-tailed t-test). **C**. Transcriptional profiling was performed on Control, Id KD, Robo1 KD and Id Robo1 KD cells. Proportional Venn diagrams (BioVenn) were generated to visualise the overlapping genes between the different comparisons. **D**. GSEA Enrichment plots of the hallmark Myc targets version 1 signature from MSigDB. NES = normalised enrichment score. **E**. Consensus Transcription factor motif analysis using the Encyclopedia of DNA Elements (ENCODE) and ChIP enrichment analysis (ChEA) data sets determined using EnrichR. The combined score is a combination of the p-value and z-score.

Figure 5: Model showing the mechanism of Id-Robo1 action in cancer cells.

The proposed model for the regulation of Myc by Id and Robo1. Co-A indicates representative Myc activator and Co-R indicates representative Myc repressor.

Table 1. Gene expression signatures of breast cancer metastasis and breast cancer stem cells. This table showed a collection of gene sets which comprised several metastatic signatures that were picked from the C2 collection on the MSigDB database and several other signatures that were manually curated. GSEA analysis was carried out to identify whether any of the Id1/3 targets from the profiling experiment are enriched in these signatures.

Study	Signature	Type	Available on GSEA MSigDB database?
Landemaine et al. A six-gene signature predicting breast cancer lung metastasis. Cancer Res. 2008 Aug 1;68(15):6092-9	Lung metastasis signature of breast cancer	Metastatic tissue tropism	Yes
Bild et al. Oncogenic pathway signatures in human cancers as a guide to targeted therapies. Nature 2006, 439:353-357.	Expression profile of 4 individual genes -- Myc, E2F3, Ras, Src, β-catenin	Signalling pathway	Yes
van 't Veer et al. Gene expression profiling predicts clinical outcome of breast cancer. Nature 2002, 415:530-536.	Poor prognosis signature of breast cancer	Classifier that classifies patients as having good or poor prognosis	Yes
Wang et al. Gene-expression profiles to predict distant metastasis of lymph-node-negative primary breast cancer. Lancet 2005, 365:671-679.	Poor prognosis signature of breast cancer	Classifier	Yes
Ramaswamy et al. A molecular signature of metastasis in primary solid tumors. Nat Genet 2003, 33:49-54.	General metastasis	Classifier	Yes
Finak et al. Stromal gene expression predicts clinical outcome in breast cancer. Nat Med 2008, 14:518-527.	Breast tumor stromal gene expression signature	Classifier	Yes
Farmer et al. A stroma-related gene signature predicts resistance to neoadjuvant chemotherapy in breast cancer. Nat Med 2009, 15:68-74.	Stromal gene expression signature of breast tumor treated with chemotherapy	Classifier	Yes

Kang et al. A multigenic program mediating breast cancer metastasis to bone. Cancer Cell 2003, 3:537-549.	Bone metastasis signature of breast cancer	Metastatic tissue tropism	No
Minn et al. Genes that mediate breast cancer metastasis to lung. Nature 2005, 436:518-524	Lung metastasis signature of breast cancer	Metastatic tissue tropism	No
Bos et al. Genes that mediate breast cancer metastasis to the brain. Nature 2009, 459:1005-1009.	Bone metastasis signature of breast cancer	Metastatic tissue tropism	No
Padua et al. TGFbeta primes breast tumors for lung metastasis seeding through angiopoietin-like 4. Cell 2008, 133:66-77.	TGF-b signature in lung metastasis of breast cancer	Signalling pathway	No
Aceto et al. Tyrosine phosphatase SHP2 promotes breast cancer progression and maintains tumor-initiating cells via activation of key transcription factors and a positive feedback signaling loop. Nat Med. 2012 Mar 4;18(4):529-37.	Shp2 signature in breast cancer metastasis	Signalling pathway	No
Minnet al. Distinct organ-specific metastatic potential of individual breast cancer cells and primary tumors. J Clin Invest. 2005 Jan;115(1):44-55.	Poor prognosis signature of breast cancer ; Breast cancer metastasis signature; Bone metastasis signature of breast cancer	Metastatic tissue tropism	No
Tang et al. Transforming growth factor-beta can suppress tumorigenesis through effects on the putative cancer stem or early progenitor cell and committed progeny in a breast cancer xenograft model. Cancer Res. 2007 Sep 15;67(18):8643-52.	TGF-b signature in lung metastasis of breast cancer	Signalling pathway	No
Liu et al. The prognostic role of a gene signature from tumorigenic breast-cancer cells. The New England journal of medicine. 2007. 356(3), 217-26.	Gene signatures of CD44+CD24-/low tumorigenic breast-cancer cell-lines and normal breast epithelium	Cancer stem cell	No
Charafe-Jauffret et al. Breast cancer cell lines contain functional cancer stem cells with metastatic capacity and a distinct molecular signature.	Breast cancer stem cell signature	Cancer stem cell	No

2009. Cancer research, 69(4), 1302-13.			
Dontu, et al. In vitro propagation and transcriptional profiling of human mammary stem/progenitor cells. 2003. Genes & development, 17(10), 1253-70.	Gene signature of human mammary stem and progenitor cells	Cancer stem cell/ Differentiation	No

Table 2. GSEA on the Intersect 1 genes from Figure 4C against the MSigDB hallmark gene sets.

INTERSECT 1 GSEA						
Gene Set Name	**# Genes in Gene Set (K)**	**Description**	**#GenesinOverlap (k)**	**k/K**	**p-value**	**FDR (q-value)**
HALLMARK_E2F_TARGETS	200	Genes encoding cell cycle related targets of E2F transcription factors.	158	0.79	5.02E-178	2.51E-176
HALLMARK_G2M_CHECKPOINT	200	Genes involved in the G2/M checkpoint, as in progression through the cell division cycle.	116	0.58	2.32E-105	5.80E-104
HALLMARK_MYC_TARGETS_V1	200	A subgroup of genes regulated by MYC - version 1 (v1).	113	0.565	7.79E-101	1.30E-99
HALLMARK_OXIDATIVE_PHOSPHORYLATION	200	Genes encoding proteins involved in oxidative phosphorylation.	96	0.48	1.04E-76	1.30E-75
HALLMARK_MYC_TARGETS_V2	58	A subgroup of genes regulated by MYC - version 2 (v2).	42	0.7241	4.60E-45	4.60E-44
HALLMARK_MTORC1_SIGNALING	200	Genes up-regulated through activation of mTORC1 complex.	66	0.33	1.70E-40	1.42E-39
HALLMARK_MITOTIC_SPINDLE	200	Genes important for mitotic spindle assembly.	60	0.3	2.76E-34	1.97E-33
HALLMARK_DNA_REPAIR	150	Genes involved in DNA repair.	51	0.34	2.54E-32	1.59E-31
HALLMARK_UNFOLDED_PROTEIN_RESPONSE	113	Genes up-regulated during unfolded protein response, a cellular stress response related to the endoplasmic reticulum.	31	0.2743	3.62E-17	2.01E-16

HALLMARK_FATTY_ACID_METABOLISM	158	Genes encoding proteins involved in metabolism of fatty acids.	35	0.2215	5.10E-16	2.55E-15
HALLMARK_ADIPOGENESIS	200	Genes up-regulated during adipocyte differentiation (adipogenesis).	39	0.195	1.08E-15	4.89E-15
HALLMARK_CHOLESTEROL_HOMEOSTASIS	74	Genes involved in cholesterol homeostasis.	24	0.3243	1.95E-15	8.11E-15
HALLMARK_ESTROGEN_RESPONSE_LATE	200	Genes defining late response to estrogen.	35	0.175	8.70E-13	3.11E-12
HALLMARK_GLYCOLYSIS	200	Genes encoding proteins involved in glycolysis and gluconeogenesis.	35	0.175	8.70E-13	3.11E-12
HALLMARK_UV_RESPONSE_UP	158	Genes up-regulated in response to ultraviolet (UV) radiation.	28	0.1772	1.18E-10	3.95E-10
HALLMARK_SPERMATOGENESIS	135	Genes up-regulated during production of male gametes (sperm), as in spermatogenesis.	25	0.1852	4.39E-10	1.37E-09
HALLMARK_ANDROGEN_RESPONSE	101	Genes defining response to androgens.	20	0.198	7.15E-09	2.10E-08
HALLMARK_ESTROGEN_RESPONSE_EARLY	200	Genes defining early response to estrogen.	28	0.14	2.76E-08	7.68E-08
HALLMARK_IL2_STAT5_SIGNALING	200	Genes up-regulated by STAT5 in response to IL2 stimulation.	25	0.125	1.31E-06	3.27E-06
HALLMARK_KRAS_SIGNALING_UP	200	Genes up-regulated by KRAS activation.	25	0.125	1.31E-06	3.27E-06

Table 3 .GSEA on the Intersect 2 genes from Figure 4C against the MSigDB hallmark gene sets.

INTERSECT 2 GSEA						
Gene Set Name	**# Genes in Gene Set (K)**	**Description**	**# Genes in Overlap (k)**	**k/K**	**p-value**	**FDR (q-value)**
HALLMARK_INTERFERON_GAMMA_RESPONSE	200	Genes up-regulated in response to IFNG [GeneID=3458].	60	0.3	3.53E-38	1.76E-36
HALLMARK_INTERFERON_ALPHA_RESPONSE	97	Genes up-regulated in response to alpha interferon proteins.	43	0.4433	4.26E-36	1.06E-34
HALLMARK_HYPOXIA	200	Genes up-regulated in response to low oxygen levels (hypoxia).	39	0.195	5.11E-18	8.51E-17
HALLMARK_P53_PATHWAY	200	Genes involved in p53 pathways and networks.	33	0.165	2.66E-13	3.33E-12
HALLMARK_APOPTOSIS	161	Genes mediating programmed cell death (apoptosis) by activation of caspases.	28	0.1739	4.49E-12	4.49E-11
HALLMARK_ESTROGEN_RESPONSE_EARLY	200	Genes defining early response to estrogen.	31	0.155	7.51E-12	4.70E-11
HALLMARK_HEME_METABOLISM	200	Genes involved in metabolism of heme (a cofactor consisting of iron and porphyrin) and erythroblast differentiation.	31	0.155	7.51E-12	4.70E-11
HALLMARK_MYOGENESIS	200	Genes involved in development of skeletal muscle (myogenesis).	31	0.155	7.51E-12	4.70E-11

HALLMARK_PROTEIN_SECRETION	96	Genes involved in protein secretion pathway.	21	0.2188	2.31E-11	1.28E-10
HALLMARK_EPITHELIAL_MESENCHYMAL_TRANSITION	200	Genes defining epithelial-mesenchymal transition, as in wound healing, fibrosis and metastasis.	30	0.15	3.77E-11	1.89E-10
HALLMARK_ESTROGEN_RESPONSE_LATE	200	Genes defining late response to estrogen.	29	0.145	1.82E-10	8.29E-10
HALLMARK_APICAL_JUNCTION	200	Genes encoding components of apical junction complex.	28	0.14	8.47E-10	3.53E-09
HALLMARK_IL2_STAT5_SIGNALING	200	Genes up-regulated by STAT5 in response to IL2 stimulation.	26	0.13	1.62E-08	5.77E-08
HALLMARK_KRAS_SIGNALING_DN	200	Genes down-regulated by KRAS activation.	26	0.13	1.62E-08	5.77E-08
HALLMARK_ALLOGRAFT_REJECTION	200	Genes up-regulated during transplant rejection.	25	0.125	6.63E-08	2.21E-07
HALLMARK_UNFOLDED_PROTEIN_RESPONSE	113	Genes up-regulated during unfolded protein response, a cellular stress response related to the endoplasmic reticulum.	18	0.1593	1.16E-07	3.62E-07
HALLMARK_ADIPOGENESIS	200	Genes up-regulated during adipocyte differentiation (adipogenesis).	24	0.12	2.60E-07	6.83E-07
HALLMARK_TNFA_SIGNALING_VIA_NFKB	200	Genes regulated by NF-kB in response to TNF [GeneID=7124].	24	0.12	2.60E-07	6.83E-07
HALLMARK_XENOBIOTIC_METABOLISM	200	Genes encoding proteins involved in processing of drugs and other xenobiotics.	24	0.12	2.60E-07	6.83E-07

HALLMARK_IL6_JAK_STAT3_SIGNALING	87	Genes up-regulated by IL6 [GeneID=3569] via STAT3 [GeneID=6774], e.g., during acute phase response.	15	0.1724	4.51E-07	1.13E-06

A.

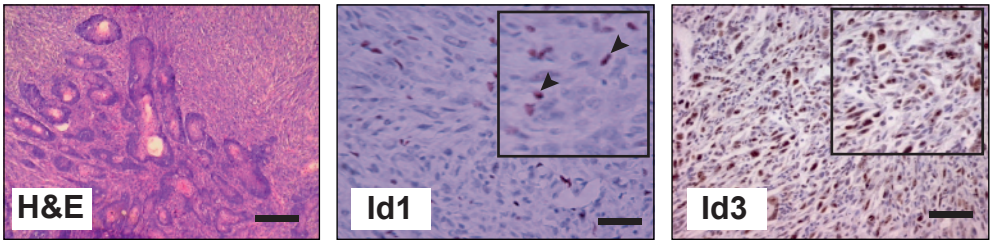

B.

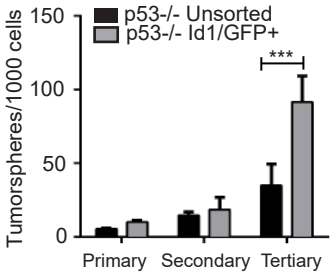

C.

Transplant round	Cell population	No. of cells			Tumour-initiating cell frequency (95% confidence interval)
		1000	100	10	
First round (from *in vivo* culture)	Id1/GFP+	9/9	4/9	1/9	1/151(1/64-1/352)
	Unsorted	10/10	2/9	0/8	1/285(1/133-1/607)
Second round (from harvested tumour)	Lin- Id1/GFP+	-	6/7	1/15	1/42(1/20-1/87)
	Lin- Id1/GFP-	-	3/10	0/10	1/314(1/102-1/970)
	Lin- Unsorted	-	4/10	0/10	1/221(1-83-1/588)

E.

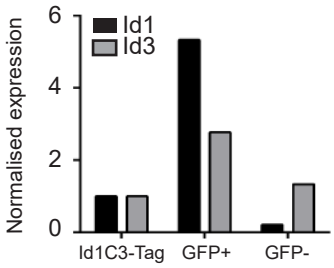

D.

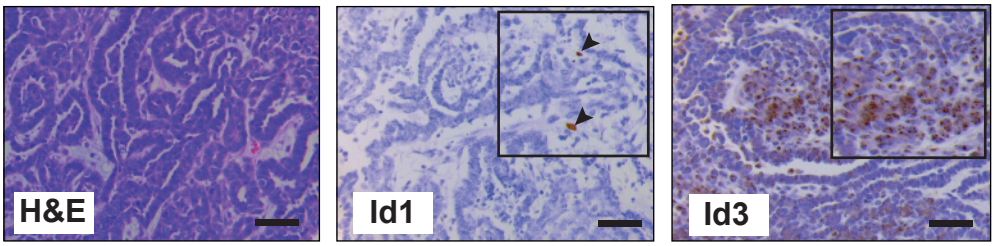

F.

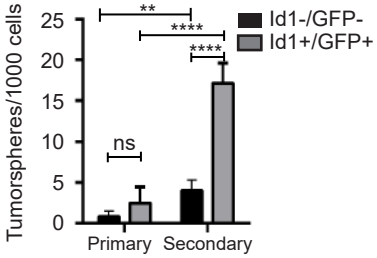

G.

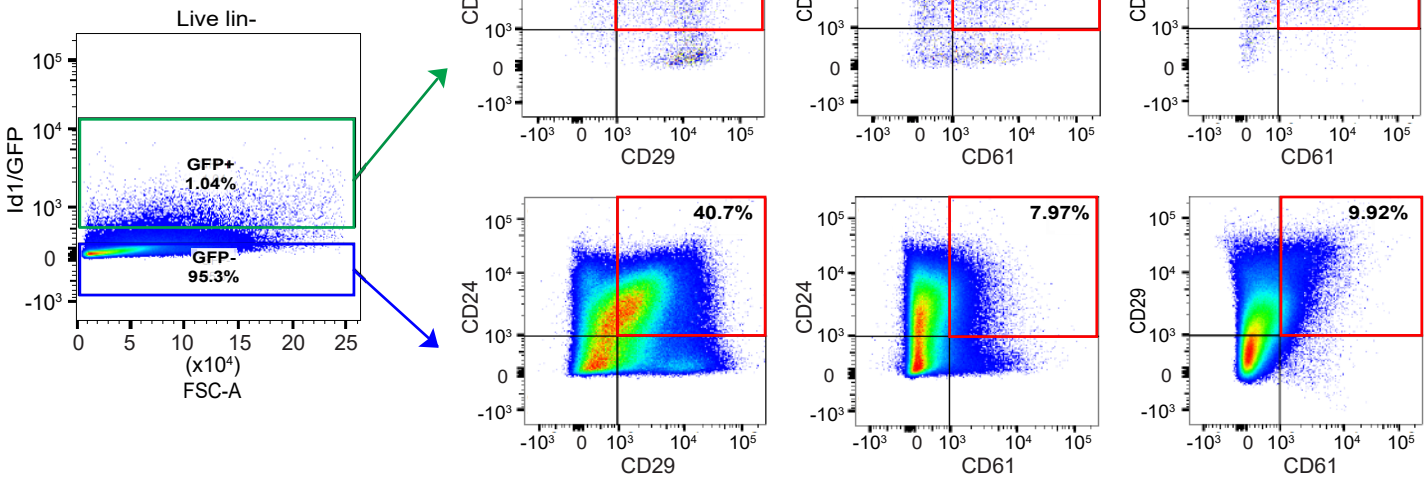

Figure 1

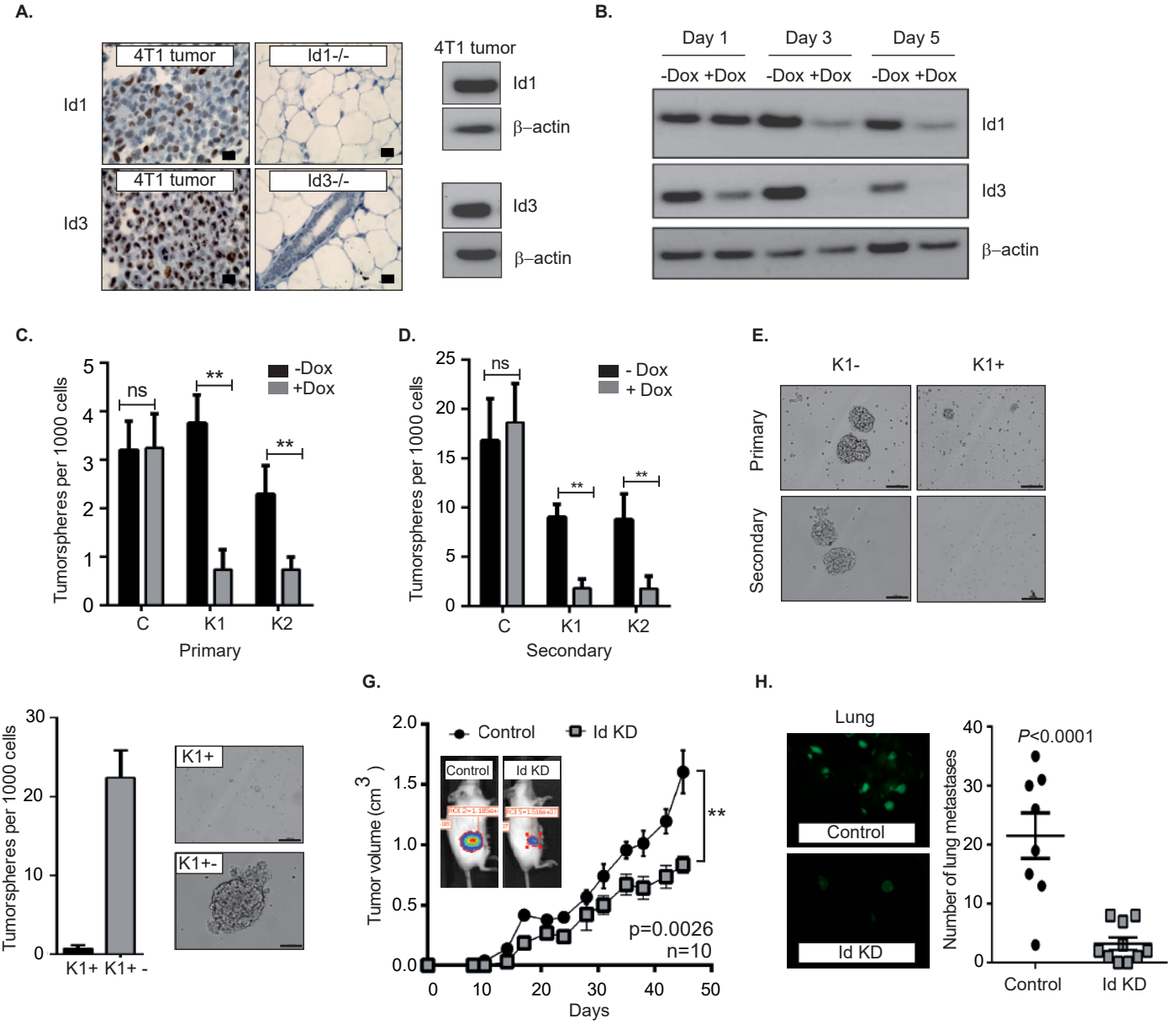

Figure 2

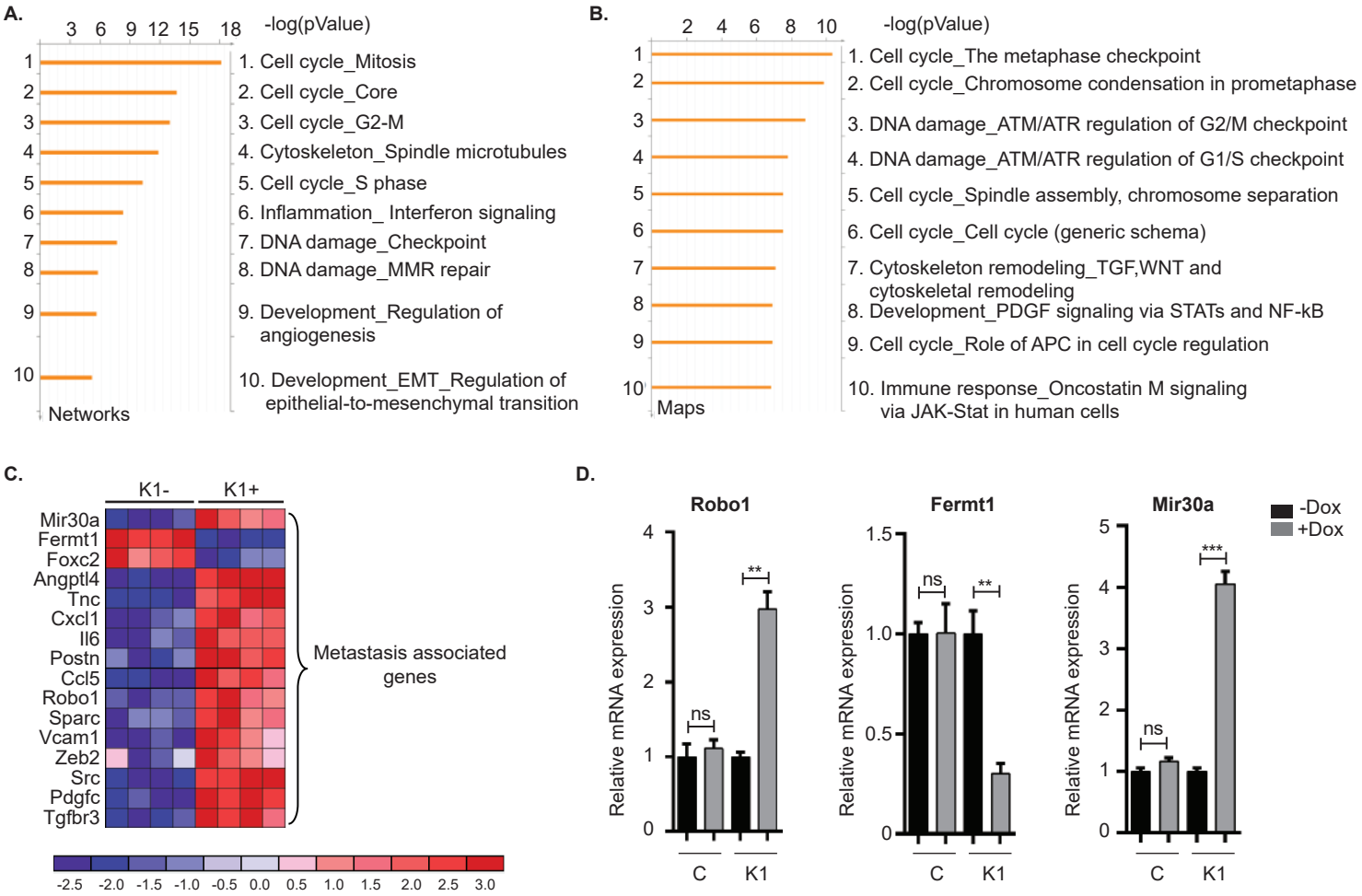

Figure 3

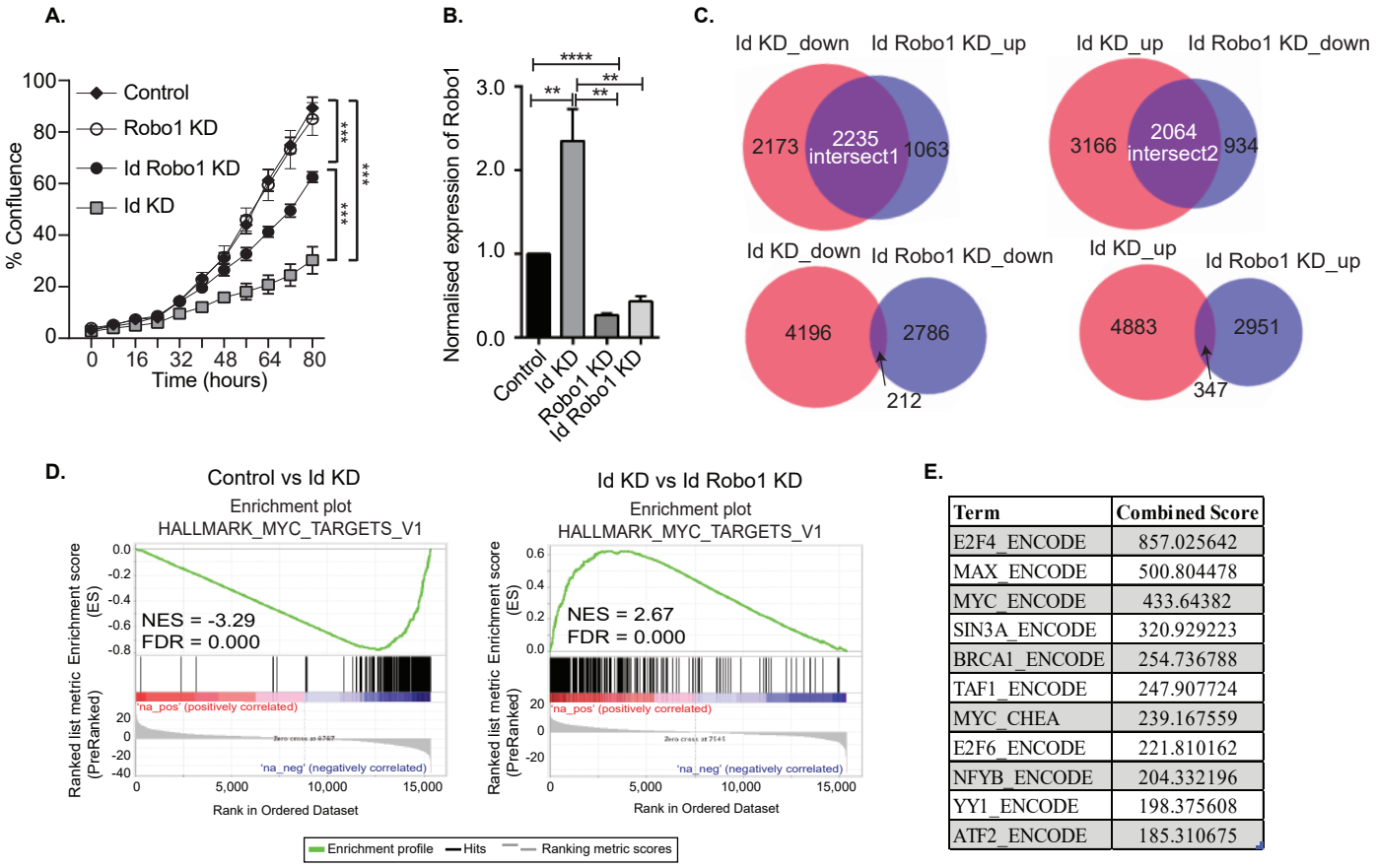

E.

Term	Combined Score
E2F4_ENCODE	857.025642
MAX_ENCODE	500.804478
MYC_ENCODE	433.64382
SIN3A_ENCODE	320.929223
BRCA1_ENCODE	254.736788
TAF1_ENCODE	247.907724
MYC_CHEA	239.167559
E2F6_ENCODE	221.810162
NFYB_ENCODE	204.332196
YY1_ENCODE	198.375608
ATF2_ENCODE	185.310675

Figure 4

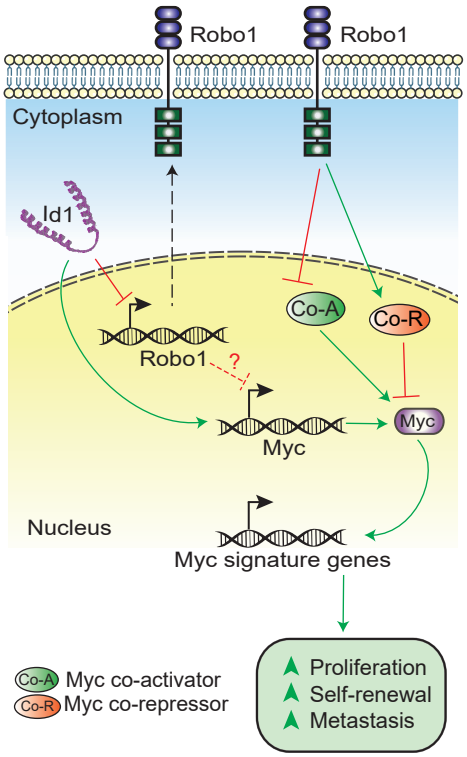
Robo1
Robo1
Cytoplasm
Id1
Co-A
Co-R
Robo1
?
Myc
Myc
Nucleus
Myc signature genes
Co-A Myc co-activator
Co-R Myc co-repressor
Proliferation
Self-renewal
Metastasis

Figure 5